Particle Coarsening in Polypropylene/Polyethylene Blends

Z. H. Stachurski*

Department of Engineering, The Australian National University, Canberra, ACT 0200, Australia

G. H. Edward, Mei Yin, and Yu Long†

Department of Materials Engineering, Monash University, Clayton, Vic 3168, Australia

Received August 8, 1995; Revised Manuscript Received December 5, 1995⊗

ABSTRACT: We report the results of particle growth in a polydisperse blend system as a function of (i) heat treatment temperature (190, 220, 250, and 280 °C) and (ii) time of heat treatment (0−290 min) for three blends of isotactic polypropylene and linear low-density polyethylene, prepared by melt extrusion. To a first approximation, the growth of the particles obeys the $t^{1/3}$ law; however, the polydispersity of the solute polymer has an effect on this relationship. The dependence on molecular weight is analyzed, and it is shown that for polydisperse solute the gradient of growth should decrease with time.

Introduction

The control of microstructures in polymer blends is of great practical significance. During processing, as in extrusion or injection molding, there are two main factors which will have an effect on microstructural changes: (i) melt flow and (ii) temperature rise. The initial result of shear or extensional flow may be homogenization and other effects such as preferred molecular orientation and induced nucleation. However this Article is concerned mainly with the temperature element of the process, that is, reheating, diffusion, and particle growth under static (no-flow) conditions. We believe that in our case the viscosity of the matrix is sufficiently high to eliminate hydrodynamic coalescence of particles.

Blends of isotactic polypropylene (iPP) and linear low-density polyethylene (PE) are known to be immiscible,[1] except in the molten state at very low levels of concentration (at either end of the composition range). It is known that these blends become transparent at the extrusion temperatures, which implies dispersion close to molecular dimensions, aided by the shear mixing. On cooling, such blends become milky, indicating light scattering by phase separation, crystallization, or both. It is certain that these blends, made with the use of a conventional single-screw extruder,[2] achieve transparency mainly through the mixing action of the shear flow. As shown later in more detail, the temperature employed during extruding was 230 °C, whereas subsequent heat treatment experiments were carried out up to 280 °C, at which growth of the PE particles was still observed. Therefore this is a case where a transparent, pseudohomogenous blend is made, and its molecular structure is stabilized by quenching and subsequent crystallization. We expect that the polymer melt never reached a truly homogenous, single phase state but, rather, that we start with a system which is already phase separated but with particle sizes below the critical size for light scattering. The kinetics of growth in this system are directly analogous to the Ostwald ripening mechanism in metals and in contrast to other cases where blends were prepared as a homogeneous single phase and particle growth required prior nucleation of the second phase or phase separation through spinodal decomposition.[3−6]

Initially in the PE/iPP blends the radius of the smallest particle is larger than the critical radius for nucleation by binodal decomposition, the radius of the largest particle is of the order of 1 μm, and this microstructure is retained in the solid state after crystallization (and vitrification if appropriate). The system is not in thermodynamic equilibrium but remains stable due to the immeasurably low diffusion rates at room temperature. When heated above the highest melting temperature (of iPP—both polymers in liquid state), but below the degradation temperature of the components of the blend, the excess interfacial free energy and the increased mobility will cause microstructural changes to take place at a measurable rate, as reported previously for this and related blend systems.[3−7]

Another important area addressed in this Article is the temperature dependence of the process. Experiments were carried out over as wide as possible temperature range to test the relationship, which involves quantities such as equilibrium solubility, interfacial tension, and diffusion coefficient. Previously published results were usually limited to one or two temperatures closely spaced[3−6] from which the temperature dependence cannot be discerned. It is important to note that Crist and Nesarikar[6] studied the relative magnitudes of growth due to diffusion and coalescence, the latter being affected mainly by matrix viscosity. In order to distinguish between the two mechanisms, they employed materials of different molecular weights to vary the matrix viscosity while keeping the temperature essentially constant. In our case varying temperature affects both the diffusion and hence the particle growth rate, as well as the matrix viscosity. We believe that in the PE/iPP blends studied here the viscosity of the matrix is sufficiently high to prevent coalescence of the particles. By contrast, Wenig[7] reported coalescence only, and this will be discussed later.

Theoretical Background. It is assumed that an equilibrium phase diagram for the blend is as shown in Figure 1. The composition of the blend, C_o, is described by the molecular concentration of the minor phase. The equilibrium solubility is denoted, C_e, and in general for the blends considered here, $C_e \ll C_o$. The Thomson−Freundlich effect predicts that the composition, C_R, of

† Present address: CRC for Polymer Blends, c/o Department of Applied Chemistry, RMIT, Melbourne, Australia.

⊗ Abstract published in *Advance ACS Abstracts,* February 1, 1996.

0024-9297/96/2229-2131$12.00/0

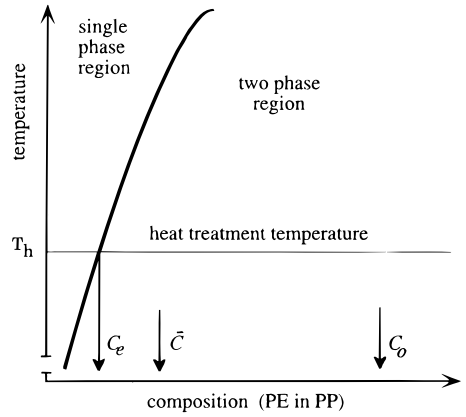

Figure 1. Portion of an equilibrium phase diagram for a binary blend in liquid state of isotactic polypropylene and linear low-density polyethylene. C_o is the composition of the blend (for example, 20PE/80iPP). Particle coarsening takes place at an experimental heat treatment temperature, T_h. C_e is the equilibrium solubility of PE in iPP at any given temperature. C is the supersaturated composition due to the presence of small particles.

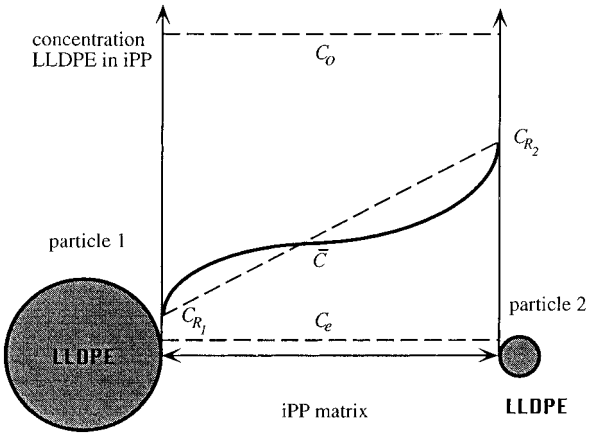

Figure 2. Concentration field of solute polymer in matrix between two particles of different sizes. The levels, C_o and C_e, refer to quantities defined in Figure 1. In equilibrium the concentration gradient is linear. However the presence of many particles of different sizes will result in a general supersaturation, C, with concentration gradients around individual particles not necessarily linear.

the solute in the matrix adjacent to a particle depends inversely on the radius, R, of the particle:[8]

$$C_R = C_e\left[1 + \left(\frac{2V_m\gamma_{int}}{kT}\right)\frac{1}{R}\right] \tag{1}$$

where KT is Boltzmann constant and absolute temperature, γ_{int} is the interfacial surface tension, and V_m is the individual molecular volume of the solute polymer chain.

In a system containing a distribution of particle sizes, the resulting composition gradient between the particles will cause a net flow of the solute polymer toward the larger particles. In a steady-state situation, the composition gradient between two particles should be linear. However, the gradients will be different between different pairs of particles, and the situation can be approximated by assuming a general level of supersaturation, $\bar{C}$, with individual particles surrounded by levels given by eq 1. This is indicated in Figure 2 by the curved line joining the two particles.

The diffusion-controlled growth theory is used here for the case of a mixture of two incompatible polymers in the liquid state. Effects due to internal strains or anisotropy may be relevant but are omitted from consideration. There are five basic assumptions. (i) There is no change of volume during particle growth (i.e., div(V) = 0). (ii) The diffusing polymer is monodispersed (i.e., all chains are of equal length). (iii) The particles diminish (or grow) at near-steady-state conditions. (iv) The particles are sufficiently far apart so that they do not interfere with each other; the diffusion field for each particle is spherically symmetric. (v) Fick's law holds for the radial rate of polymer diffusion.

Kinetics of Growth. It follows from assumptions iii, iv, and v that the change of an individual particle radius during growth, dR_i, is determined by the rate of polymer flow:

$$dR_i = -JV_m\,dt \tag{2}$$

where J is the flux rate given by Fick's law. Combined with eq 1 this results in the following relationship for each particle:[9]

$$dR_i = D\frac{2V_m^2\gamma_{int}C_e}{kT}\frac{1}{R_i^2}\left[\frac{R_i}{R_C} - 1\right]dt \tag{3}$$

where D is the diffusion coefficient. Equation 3 is in accordance with the arguments satisfying the conditions that $dR_i/dt > 0$ for $R_i > R_C$ and $dR_i/dt < 0$ for $R_i < R_C$, where R_C is the critical particle radius for which $\bar{C} - C_R = 0$.

If the initial distribution of particle sizes is unimodal, then the average particle size, $\bar{R} = \Sigma R_i/\Sigma i$, defines the position of the peak on a graph of particle numbers versus particle size. Lifschitz and Slyozov obtained the following solution for the growth of the average particle size:[9]

$$(\bar{R})^3 = (\bar{R}_o)^3 + \frac{8}{9}\left[\frac{V_m^2\gamma_{int}C_e}{kT}D\right]t \tag{4}$$

where $R = R_o$ at $t = 0$.

Temperature Dependence. Three parameters in eq 4 vary with temperature: D, C_e, and γ_{int}. The diffusion coefficient is strongly temperature dependent,[10,11] whereas γ_{int} and C_e are only weak functions of temperature, and more importantly, their dependence in this blend system is of opposite sense, that is, if one decreases then the other increases. Therefore it can be assumed that the product, $C_e\gamma_{int}$, is to a first approximation temperature independent.

The heat treatment temperature (at which the particles are made to grow) is well above the glass transition and melting temperatures of both polymers. Therefore it can be assumed that the temperature dependence of diffusion will follow the Arrhenius relationship:

$$D = D_o\exp(-E_D/kT) \tag{5}$$

where E_D is the diffusional activation energy and D_o is a constant.[11,12] Using this relationship, eq 4 can be represented as:

$$(\bar{R})^3 = K(T)t + (\bar{R})_o^3 \tag{6}$$

where

$$K(T) = \left[\frac{8V_m^2\gamma_{int}C_eD_o\exp(-E_D/kT)}{9kT}\right] = \frac{A}{T}\exp\left(\frac{-B}{T}\right) \tag{7}$$

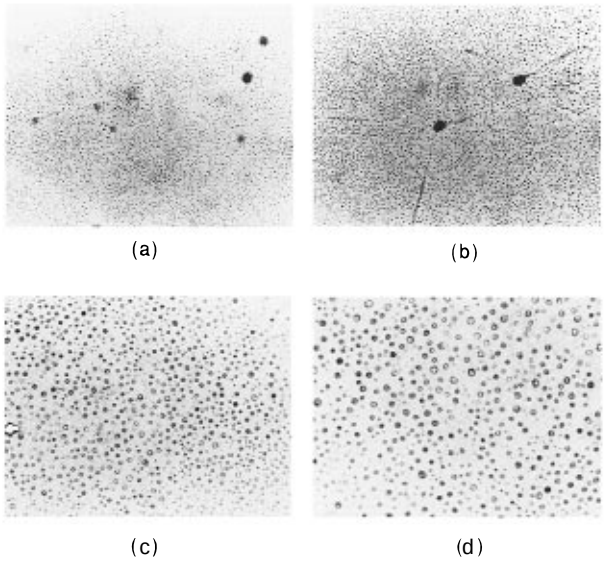

Figure 3. Optical micrographs: (a) initial 20/80 blend after extrusion and (b−d) heat treated at 220 °C for 3, 25, and 60 min. Notice that the PE particles appear inside the iPP spherulites, the boundaries of which are clearly visible in a and b.

If R^3 is plotted against time, eq 7 predicts that it should be a straight line, with the gradient of the line, $K(T)$, being a strong exponential function of temperature, and the positive intercept at $t = 0$ being the mean particle size cubed at the onset of heat treatment $(R_o)^3$. The parameters A and B should be constant for a given system which satisfies all the assumptions listed above.

Experimental Section

Starting Materials and Blend Preparation. The starting materials were commercial polymers obtained from ICI Australia: isotactic polypropylene (ρ = 0.905 g/cm^3, M_w = 57 000) and linear low-density polyethylene (ρ = 0.919 g/cm^3, M_w = 30 300, M_n/M_w = 3.7). They were used with typical additives present. The blends were prepared by tumble-blending the polymer granules for 15 min and then melt-blending in a 1.5 in. Johns single-screw extruder using a temperature profile varying from 190 to 230 °C, for zones 1−4 from the feed to the die. Then followed quenching in water, blow drying, and finally granulation.[2] For reference, pure iPP was also was passed through an identical process of extrusion so as to give it the same history as the blend samples. Three separate blends were prepared, blends 1 and 2 both of composition 20% PE to 80% iPP and blend 3 of composition 10% PE to 90% iPP by volume.

Samples of the blends were compression molded from the granules in an instrumented hot platen press in the form of sheets 15 cm × 15 cm × 2 mm. The sheets were heated to the following temperatures: T_h = 190, 220, 250, and 280 °C. Four sheets were prepared at each composition and temperature and held in the mold for increasing lengths of time. In order to avoid oxidation, the materials were enclosed in aluminum foil. After holding the samples in the press, they were quenched to room temperature in cold water. No solvents of any kind were used during the preparation of the samples.

Measurement of Particle Size. A polarizing optical microscope (Olympus BH-2) with a hot stage (Mettler-FP80) was used to observe the morphology and to measure the iPP spherulites and PE particle sizes. The experimental procedure involved the cutting of a 10−15 μm thick film from the samples using a ultramicrotome, placing the film samples between two glass slides, and heating to 120 °C, at which temperature PE was molten but iPP was still in the solid state. Melting of PE increased the contrast between the two polymers and made their observations possible. Since the film thickness was at least 1 order of magnitude greater than most particle sizes, the microscopic view closely approximated the actual distribution of particles in the bulk and made it unnecessary to use size distribution-estimating methods such as the Schwartz−Soltyakov[13] method as were required in other cases.[3−6] The image was recorded on a photographic film, and the micrographs were digitized on a Macintosh IIcx computer with an Apple scanner. The resolution of 300 dpi was used. An image analysis program, IMAGE(1.4), was used to analyze the digitized images.

In the measurement of the first (20/80) blend, any objects (particles) <1 μm in diameter were cut off from counting. In the second (20/80) and third (10/90) blends, the lower limit cutoff was lowered to 0.5 μm.

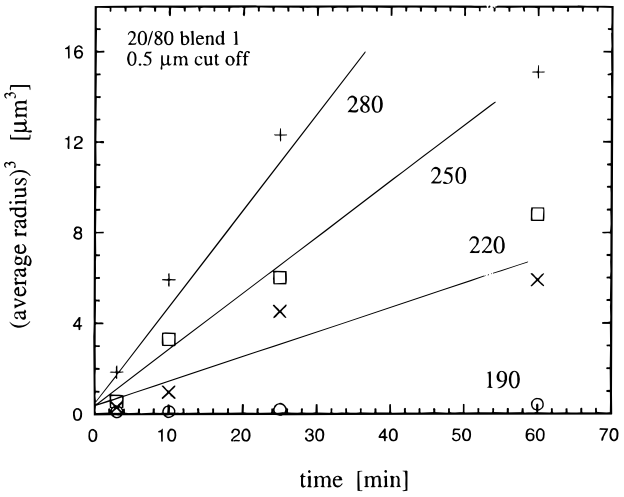

Figure 4. Variation of average particle radius raised to the power of 3 versus time and temperature of heat treatment for the 20/80 (1.0 μm cutoff) blend 1.

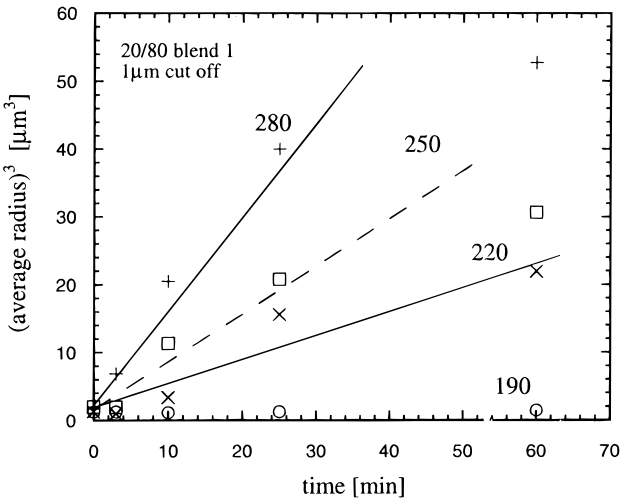

Figure 5. Variation of average particle radius raised to the power of 3 versus time and temperature of heat treatment for the 20/80 (0.5 μm cutoff) blend 1.

Results and Discussion

Morphology and Particle Sizes. In Figure 3 are shown optical micrographs from one of the 20/80 blends. The first micrograph shows a very fine dispersion of PE in iPP, typical of the blend obtained after extrusion. The next three micrographs show the changing morphology of the PE particles in the blend heat treated at 250 °C for 3, 25, and 60 min. The increasing size of the particles with annealing time and temperature was observed in all samples. The outlines of the iPP spherulites are clearly visible in a and b. The spherulites could be easily observed under lower magnification

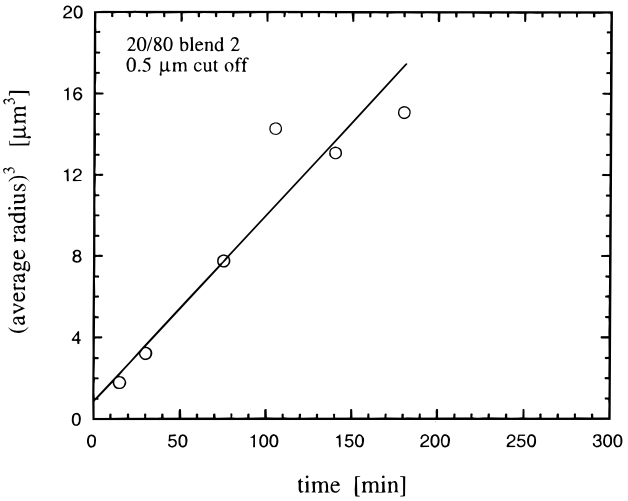

Figure 6. Variation of average particle radius raised to the power of 3 versus time and temperature of heat treatment for the 20/80 (0.5 μm cutoff) blend 2.

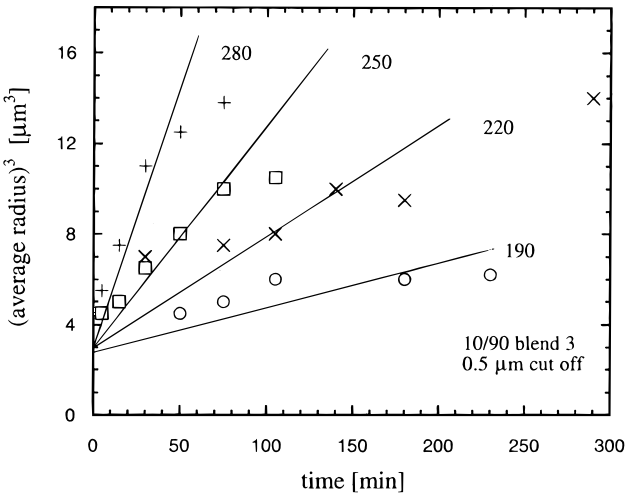

Figure 7. Variation of average particle radius raised to the power of 3 versus time and temperature of heat treatment for the 10/90 (0.5 μm cutoff) blend 3.

and polarized light condition, and the sizes of the spherulites were measured. The spherulite sizes in pure iPP and the blends were essentially the same for a given temperature and annealing time.

The PE particles are also spherulitic. Each particle was found to be a single spherulite except those above about 5 μm, in which occasionally two or three spherulites were observed. This small size of spherulites is not unusual since the nucleation density in PE is generally much higher than that in iPP. The average radii of the particles, determined by the digital analysis method, are plotted against heat treatment time in the graphs shown in Figures 4−7.

Equilibrium Solubility of PE in iPP. An equilibrium phase diagram for the binary mixture of iPP and PE has not been determined yet. We have made the reasonable assumption that it is of the upper critical transition point type, with the range of temperatures and composition studied here falling into the two-phase region. It is, therefore, assumed that C_e is a slowly increasing function of temperature as shown in Figure 1. The dependence of the equilibrium solubility, C_e, on temperature can be obtained formally by solving the general thermodynamic equation:[8]

$$\frac{d\Delta G_m(T)}{dC_e(T)} = 0 \tag{8}$$

where ΔG_m is the excess free energy of mixing of the two polymers. Simple calculations of the excess free energy of mixing using the Flory−Huggins model corroborate the above assumption as to the temperature dependence of C_e; however, the parameters used in the model are not known with sufficient accuracy to give reliable quantitative predictions. To the best of our knowledge, no experimentally determined variation of equilibrium solubility of PE in iPP for this blend is available at this stage.

Interfacial Energy. The surface energy of polymers decreases slowly with temperature according to the semiempirical equation:[14,15]

$$\gamma = \gamma_o(1 - T/T_c)^n \tag{9}$$

where $\gamma_o = \gamma$ at 0 K, T_c is a critical temperature, and the exponent n is close to unity. Since the molecular

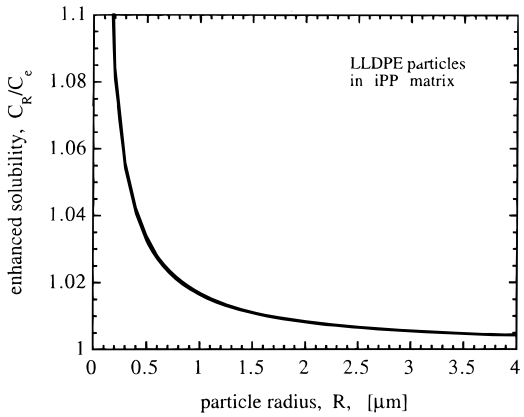

Figure 8. Plot of enhanced solubility as a function of particle radius for PE in iPP according to eq 1 and data given in the text.

interactions between the two polymers involve dispersive forces only, the Flory interaction parameter, χ, will also decrease with temperature:[16,17]

$$\chi = \frac{k_1}{T} - k_2 \tag{10}$$

where k_1 and k_2 are constants. Consequently it can be concluded that the interfacial energy between PE and iPP, $\gamma_{int} \approx \chi^{1/2}$, will also decrease with temperature. This is consistent with the view that solubility increases with temperature.[16−18]

The dependence of enhanced solubility on particle radius, expressed by the ratio C_R/C_e, is shown in Figure 8. The following values were used in eq 1: V_m = DP × volume of monomer, DP = 30300/14, volume of CH_2 monomer = 26×10^{-30} m^3 (ref 10), $\gamma_{int} = 1.1$ mJ/m^2 (ref 19), $T = 493$ K, and $k = 1.38 \times 10^{-26}$ J/K. Figure 8 shows that the solubility of particles with radius smaller than 0.2 μm increases rapidly with decreasing size. Temperature variation between 463 and 553 K (190 and 280 °C, respectively) has only a small effect on this plot.

Molecular Weight Dependence Analysis. Both polymers comprising the blend are polydisperse. Since diffusion is inversely dependent on the square of molecular weight,[20−22] the shortest polymer chains of the solute will have the fastest flow rate and, in accordance with eq 2, will contribute to the growth of the larger

Table 1. Gradients, *K(T)* (in μm^3/min), Obtained from Plots Shown in Figures 4−7

temperature, KCl	80/20 blend 1		80/20 blend 2, 0.5 μm cutoff	90/10 blend 3, 0.5 μm cutoff
	1.0 μm cutoff	0.5 μm cutoff		
553 (280)	1.38	0.41		0.23
523 (250)	0.71	0.24		0.097
493 (220)	0.36	0.1	0.09	0.05
463 (190)	0.03	0.01		0.017

particles long before chains of higher molecular weight, which will take much longer time to diffuse. Therefore the diffusional flow rate, in terms of the number of individual molecular chains, will be the highest at the onset of the process and decrease with time. The effect of this on the growth rate is resolved as follows. If species of one particular molecular weight arrive at an individual particle, its radius will increase in accordance with:

$$R_{M_i}^3 = R_o^3 + \frac{8\gamma_{int} C_e V_m^2 D}{9kT} t \qquad (11)$$

Since $D \approx 1/(M_i)^2$ and $V_m \approx M_i$, one can at first assume that R_{M_i} is independent of molecular weight. The key argument is that DV_m^2 = constant with respect to variations in molecular weight; shorter chains arrive at a faster rate but contribute less toward volumetric growth, and the converse is also true. It does mean, however, that the physical and chemical compositions of the particle change continuously with time during the growth process. However both C_e and γ_{int} are also functions of molecular weight, of which the former has a very strong dependence on molecular structure. Calculations for a blend of HPB in PE show variations of many orders of magnitude[6] caused by both variations in molecular chain length and branching of the solute polymer. For interfacial surface tension, the dependence on molecular weight is of the form:[16] $C_1 - C_2(M_n)^{-z}$, with $z = 2/3$, which becomes essentially invariant for polymers with degree of polymerization > 10^3, as is the case here.

Let the distribution of molecular weights of the solute polymer be given by the function $N(M_i)$. Then if species of varying molecular weights arrive at a particle, its radius will be given by the average of the incremental increases due to the arrival of molecules of different size:

$$\bar{R}_M^3 = \frac{\int R_{M_i}^3 N(M_i)\, dM_i}{\int N(M_i)\, dM_i} \qquad (12)$$

Note that this average is for one particle, calculated with respect to varying molecular weights, and different from the average of all particles as given by eq 4. Substitution of eq 11 into 12, and noting that $\int N(M_i)\, dM_i = 1$ gives:

$$\bar{R}_M^3 = R_o^3 + \frac{8V_m^2 D\gamma_{int} t}{9kT} \int C_e(M_i) N(M_i)\, dM_i \qquad (13)$$

The final conclusion is that in blend systems with polydisperse solute polymers the growth of individual particles will not be a linear function of time but will slow down. The individual particle gradient, K_M, will decrease with time because the integral containing C_e will decrease due fractionation of molecular weight species with time, and therefore the gradient $K(T)$ of eq 6 will also decrease with time. This effect is evident in Figures 4−7, although we have drawn straight lines through the data points not knowing explicitly the form of this dependence.

Table 2. Comparison of Growth Gradients and Related Data for Several Blends

blend, matrix/ solute	solute concentration	M_w, kg/mol		temperature, K	gradient, K, μm^3/s	ref
		matrix	solute			
iPP/LLDPE	0.2	59	30	463	1.6×10^{-4}	this work
iPP/EPR	0.18	36	113	466	1.1×10^{-4}	3
PE/HPB	0.1	129	44	433	1.1×10^{-5}	6
HDPE/HPB	0.1	160	111	450	4.8×10^{-6}	4
OPE/CoPE	0.1	35	40	415	2.1×10^{-4}	5

Particle Growth Discussion. The experimental results shown in Figures 4−7 are plotted in accordance with eq 7. The straight lines fitted to the data indicate reasonable agreement with Ostwald ripening mechanism during the initial stages followed by a leveling off of the growth rate at longer times. The gradients have been measured and are given in Table 1.

The gradients, $K(T)$, for a number of blend systems have been measured and reported in several recent publications,[3−6] and Table 2 shows a comparison of their values. The growth process is very dependent on temperature and molecular weight, and for that reason these quantities are included in the table as well. The value of K for the iPP/EPR blend[3] is very close to the value obtained by us for the iPP/LLDPE blend, as expected since the measurements were carried out at similar temperatures and blend compositions. The large difference between the molecular weights of the two solutes should have no effect on diffusion according to the argument presented above but implies greater solubility of EPR in iPP as compared to LLDPE by a factor of ca. 3.5. It is to be noted, however, that in the second paper[4] Mirabella quotes the calculated value for K as 4.8×10^{-5} μm^3/s, which is 1 order of magnitude lower than that measured off Figure 3 in ref 3. Hill and Barham[5] also refer to that figure and quote a value for K as 3.8×10^{-4} μm^3/s (0.0727 $\mu m/s^{-1/3}$). The reason for the discrepancies is not known.

It is interesting to compare the HPB/PE blends which show a factor of more than 2 between their respective K values.[4−6] The blends have similar matrix materials and identical concentrations, and the HPB polymer was of the same origin in both cases. Since all the molecular parameters appear to be the same, one is forced to conclude that it is the measurement of the particle sizes and their distribution, which is the most inaccurate process, leading to discrepancies.

Wenig and Meyer[7] reported previously the growth of particles in a similar polymer blend, and their results showed a linear relationship between the particle mean diameter and time. It was reported that a unimodal distribution of particle sizes at 220 °C changed to bimodal at 280 °C and that the process of growth was not yet finished after 50 min. They proposed that growth occurred as a result of coalescence of two or more droplets, similar to that reported by Crist and Nesarikar, but the time dependence was not of the expected form.[6] We have not found any direct evidence for this behavior when observing the growth of particles under the microscope. Furthermore iPP has a much higher intrinsic viscosity compared to PE, which supports the above observation. However we cannot exclude entirely the possibility of it occurring, especially since experiments were carried out at a range of temperatures up to 280 °C.

Table 3. Experimentally Determined Paramters *A* and *B*, Defined in Eq 7

	80/20 blend 1		
	1.0 μm cutoff	0.5 μm cutoff	90/10 blend 3, 0.5 μm cutoff
A (K μm^3/min)	95×10^6	52×10^6	208×10^6
B (K)	6500	6800	7900

In eq 7, the molecular quantities that are involved in the process of diffusion are combined into the parameters A and B. These parameters can be evaluated from the experimentally determined gradients by means of the following formulae:

$$B = \frac{T_1 T_2}{T_2 - T_1}\left[\ln\left(\frac{T_2}{T_1}\right) - \ln\frac{K(T_1)}{K(T_2)}\right]$$

and

$$A = K(T)T\exp(B/T) \qquad (14)$$

Using the data from Table 1 and the above formulae, the parameters A and B were evaluated, and the average values are shown in Table 3. Next these values were used in eq 7 to plot the variation of gradients with temperature, as shown in Figure 9. The plot includes points of the experimentally determined gradients, and the fit is reasonably good. The general observations that can be made here are (i) the value of the parameter A changes markedly depending on the particle-counting process and blend composition and (ii) the value of the parameter B is, to a first approximation, constant. The average value is 7×10^3; multiplying it by the gas constant, R, one obtains the activation energy of diffusion of $E_D \approx 58$ kJ/mol. This is a rather large value as compared to 21 kJ/mol obtained from direct experimental measurements[12] and may be the result of polydispersity of the polymers.

Estimation of Errors. A serious source of error is the relatively long ramping time to reach the heat treatment temperatures and cooling times (correspondingly). To reach 280 °C from 20 °C took ca. 7 min, and cooling the mold to room temperature took 3 min. This thermal history must have a measurable effect in samples heated for short times, and therefore we allowed for an error of +2 min for each sample.

The sources of errors in the measurement of particle sizes are (i) the size of sample (number of particles and area), (ii) the selection of boundaries between particles and matrix, (iii) the uncertainty in magnification and enlargement, and (iv) the high and low cutoff values in the size distribution. In addition, the thickness of the observed layer under the microscope will be another factor.

For error i, given the size of the field of view and the number of particles observed in it, the statistical error is of the order of 2%. With respect to error ii, the calculation of radius, $R = D/2$, is carried out on the digitized image, where the distinction between matrix, particles, and boundaries is measured in terms of the level of gray scale (from white to black). In the early stages of growth (Figure 3a,b) the particles appeared black but later became transparent with pronounced black boundaries (Figure 3c,d). In the optical image the boundary lines have a finite thickness. The thickness of the boundary line can be due to at least two effects: (i) an optical effect of a spherical particle of refractive index n_p imbedded in a slab of matrix of refractive index n_m, where $n_p < n_m$, and (ii) a diffuse interface layer due to mutual interpenetration of the two polymers.[23−25] We consider the first effect to be dominant and chose the boundary to be on the outer limit of the boundary lines, which also allowed for consistency in parts a−d of Figure 3. We estimate the possible errors in diameter for small particles (<1 μm) to be as much as 25%, reducing to 10% or less for the large particles (>1 μm). The spherulite boundaries and other large or small features were excluded from calculations. The sizes of particles plotted are on the upper bound of error limits.

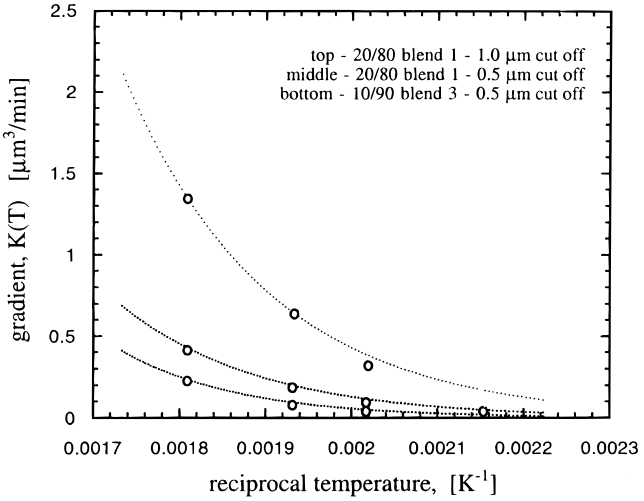

Figure 9. Plot showing the measured variation of gradients as a function of temperature. Curves drawn according to eq 7 with values of A and B from Table 2. Points represent experimentally determined gradients, shown in Table 1.

The different cutoff applied (1 and 0.5 μm) for the two 20/80 blends was found to affect the slope $K(T)$. It was found that the slopes for the blend for which a 1 μm cutoff was used, when reduced by a factor of 0.66, are approximately equal to the slopes for the blend with a 0.5 μm cutoff. Since the particle size distribution changes with time, the position of the cutoff limit will effect the calculated average radius.

Conclusions

The measruement of diffusional particle growth in blends with large polydispersity adds another element of complexity to the process and makes its quantitative evalution much more difficult. Even in monodisperse systems the quantitative agreement between the gradients measured experimentally and those predicted from theory (using independently obtained molecular quantities) is not adequate, with a discrepancy of a factor of 5 quite common. However the reported results in published literature are but few, and it is hoped that with better understanding of all the parameters involved in the process more accurate prediction of the growth rates can be achieved.

An important result is obtained from the analysis of the effect of molecular weight dependence on the rate of particle growth. The mutual canceling effect, of the molecular volume and diffusional coefficient, eliminates two quantities from the theoretical relationship. Of the remaining quantities, γ_{int} is to a large degree molecular weight independent, but C_e shows strong dependence and may decrease by orders of magnitude with increasing molecular weight. During the diffusional growth a temporary segregation of solute molecules occurs because the shorter polymer chains diffuse first, thus decreasing the average molecular weight in the large

particles (the sinks) and increasing the average molecular weight in the smaller particles (the sources). Consequently C_e for the small particles will decrease continuously, resulting in reducing gradient, $K(T =$ constant), as evident from eqs 13, 6, and 4. This analysis of the molecular weight dependence of the process predicts slowing down of the growth rate at longer times, quite separate from the natural phenomenon of "exhaustion" of particles.

Finally, an accurate measurement of the particle growth is fraught with difficulties, and large uncertainties are to be expected. These uncertainties result not only from stereological factors but also from the definition of particle size surrounded by an "interface" layer where mutual diffusion of the solute and matrix chains takes place. The evidence for the layer is clearly seen not only in this work but also in previous publications.[3−6]

Acknowledgment. We are grateful to Dr. H. R. Brown for helpful discussions on the aspects of solute/matrix interface. Y.L. and M.Y. acknowledge that research was supported by an Overseas Postgraduate Research Scholarship (OPRA) and Monash Postgraduate Scholarship (MGS). Some of the blends were prepared by V. Flaris using ICI Australia equipment.

References and Notes

(1) Utracki, L. A. *Polymer Alloys and Blends*; Hanser Verlag: Munich, 1991.
(2) Flaris, V.; Stachurski, Z. H. *J. Appl. Polym. Sci.* **1992**, *45*, 1789.
(3) Mirabella, F. M. *J. Polym. Sci., Part B* **1994**, *32*, 1205.
(4) Mirabella, F. M.; Barley, J. S. *J. Polym. Sci., Part B* **1994**, *32*, 2187.
(5) Hill, M. J.; Barham, P. J. *Polymer* **1995**, *36*, 3369.
(6) Crist, B.; Nesarikar, A. R. *Macromolecules* **1995**, *28*, 890.
(7) Wenig, W.; Meyer, K. *Colloid. Polym. Sci.* **1980**, *258*, 1009.
(8) Swalin, R. A. *Thermodynamics of Solids*; John Wiley & Sons: New York, 1962.
(9) Lifschitz, J. M.; Slyozov, V. V. *J. Phys. Chem. Sol.* **1961**, *19*, 35.
(10) Wunderlich, B. *Physics of Polymers*; Academic Press: New York, 1976; Vol. 1.
(11) Manning, J. R. Theory of Diffusion. Diffusion, American Society for Metals Seminar, OH, 1972.
(12) Bartels, C. R.; Crist, B.; Graessley, W. W. *Macromolecules* **1984**, *17*, 2702.
(13) DeHoff, R. T.; Rhines, F. N., Eds. *Quantitative Microscopy*; McGraw-Hill: New York, 1968.
(14) Hannay, N. B. *Treatise on Solid Sate Chemistry*; Plenum Press: New York, 1976; Vol. 6A, Surfaces I.
(15) Wu, S.-H. *Polymer Interfaces and Adhesion*; Marcel Dekker: New York, 1982.
(16) Anastasiadis, S. H.; Garncarz, I.; Koberstein, J. T. *Macromolecules* **1988**, *21*, 2980.
(17) Bates, F. S. *Science* **1991**, *251*, 898.
(18) Helfand, E. *Macromolecules* **1992**, *25*, 1676.
(19) Brochard-Wyart, F. In *Fundamentals of Adhesion*; Lee, T. D., Ed.; Plenum Press: New York, 1988.
(20) Kausch, H. H.; Tirrell, M. *Annu. Rev. Mater. Sci.* **1989**, *19*, 341.
(21) Klein, J. *Science* **1990**, *250*, 640.
(22) Wang, S.-Q.; Shi, Q. *Macromolecules* **1993**, *26*, 1091.
(23) Jordan, E. A.; Ball, R. C.; Donald, A. M.; Fetters, L. J.; Jones, R. A. L.; Klein, J. *Macromolecules* **1988**, *21*, 235.
(24) Kryszewski, M.; Galeski, A.; Pakula, T.; Grebowicz, J. *J. Colloid Interface Sci.* **1973**, *44*, 85.
(25) Letz, J. *J. Polym. Sci., Part A2* **1969**, *7*, 1987.

MA9511560